Macromolecules
COMMUNICATION TO THE EDITOR
pubs.acs.org/Macromolecules

Well-Ordered Lamellar Microphase-Separated Morphology of an ABA Triblock Copolymer Containing a Main-Chain Liquid Crystalline Polyester as the Middle Segment

Ryohei Ishige, Toshinari Ishii, Masatoshi Tokita,* Maito Koga, Sungmin Kang, and Junji Watanabe

Department of Organic and Polymeric Materials, Tokyo Institute of Technology, Ookayama, Meguro-ku, Tokyo 152-8552, Japan

S *Supporting Information*

Liquid crystal (LC) block copolymers composed of LC and isotropic blocks are interesting because of the following two aspects. First, the LC orientation induced by an external field can induce macroscopic orientation of the microdomains. The microdomains are following the mesogens orientation to minimize the director distortion. Large area amorphous cylinder alignments in LC block copolymers have been accomplished by application of a magnetic field.[1−3] The anchoring of the LC relative to the substrate induced orientations of lamellae or amorphous cylinders in the ultrathin films.[4] Under shear flow, a smectic LC aligns the layer normal parallel to the velocity gradient direction, so the microcylinders immersing in the smectic LC matrix have to compromise on their orientation so as to lie in the velocity gradient direction though they cannot avoid being tilted by the deformation.[5] Second, the LC can affect the microdomain morphology. On the transition from isotropic to nematic phases in the LC polymer segments, the amorphous segments changed their shape from sphere into cylinder so as to avoid LC director distortion.[6] Smectic LC block copolymers formed lamellar morphology at unusually low LC compositions.[7] In some smectic LC block copolymers, the lamellar spacing increased with decreasing temperature in the LC temperature region corresponding to the change of LC segment configuration from random coil to more extended in the lamellar normal direction.[8−10] In these copolymers, the LC segments are side-chain type in which the mesogenic moieties are connected to the polymer backbone by flexible spacers. LC block copolymers having main-chain type LC segments in which the mesogenic moieties are connected by alkylene spacers to be embedded in the chain backbone were also prepared; however, they were confronted with significant problems that the polymerization yielded the homopolymers and unintended block arrangements as well as the block copolymers.[11−13] The morphology has not been reported although their thermal transitions were well attributed to that of each segment and suggested that the LC and amorphous segments segregated strongly from each other.

In this study, we report on an ABA triblock copolymer consisting of poly(methyl methacrylate) (PMMA) as amorphous end blocks (A) and main-chain LC polymer of BB-5(3-Me) as the LC central block (B). These two types of segment were segregated each other to form lamellae which showed a clear small-angle X-ray scattering (SAXS) profile. Combining of the wide-angle X-ray diffraction pattern and an analysis of the SAXS profile demonstrates that the BB-5(3-Me) segment with 52 nm in contour length formed smectic layers lying parallel to the lamella having a thickness of 11.6 nm. It clearly shows that the LC polymer chains in the smectic phase are folded at every seven repeat units.

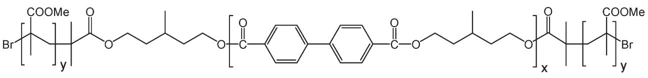

The block copolymer was prepared by atom transfer radical polymerization (ATRP) of methyl methacrylate with the Br-terminated BB-5(3-Me) as the macroinitiator (the details are described in Supporting Information). The degrees of polymerization (DP) of the BB-5(3-Me) segment (x) and the sum of the two PMMA segments ($2y$) were estimated to be 32 and 73, respectively, by ^{1}H NMR spectra. The number-average molecular weights M_n of the BB-5(3-Me) and PMMA segments are thus calculated to be 10 500 and 7300, respectively. The polydispersities (M_w/M_n) of the BB-5(3-Me) segment and the block copolymer were estimated to be 1.7 and 1.5, respectively, by gel permeation chromatography. The volume fractions of PMMA and BB-5(3-Me) segments were estimated to be 44 and 56 vol %, respectively, by the densities measured to be 1.19 and 1.33 g cm^{-3} at 20 °C by means of a pycnometer.

The LC segments in the block copolymer were well segregated with the PMMA segments and showed phase transitions similar to that observed for the precursor hydroxy-terminated BB-5(3-Me). Like the BB-5(3-Me) polyester forming a smectic C$_A$ (SmC$_A$) LC,[14] the hydroxy-terminated BB-5(3-Me) showed a jump in the heat capacity (C_P) and an endotherm peak at 25 and 145 °C, respectively, in the heating DSC thermogram (Figure 1a). Therefore, these are attributed to the glass transition and isotropization of the SmC$_A$ LC. The thermogram of the triblock copolymer (Figure 1c) is similar to that of the precursor polymer in including a jump and a peak at 35 and 141 °C, respectively, while another jump in C_P the heat capacity appears at 106 °C, which is attributable to the glass transition for PMMA block, indicating that the two types of segment were segregated from each other to display each individual thermal property. The BB-5(3-Me) segment thus transformed from glassy SmC$_A$, SmC$_A$, and isotropic liquid phases in order of increasing temperature. The isotropization enthalpy (ΔH_i) of the BB-5(3-Me)

Received: February 22, 2011
Revised: April 17, 2011
Published: May 18, 2011

block was 2.6 kJ mol^{-1}, which is three-fourths of $\Delta H_i = 3.4$ kJ mol^{-1} of the hydroxyl-terminated BB-5(3-Me).

The type of the mesophase was well identified by the X-ray diffraction pattern. Figure 2a shows the 2D WAXD fiber pattern of the triblock copolymer (Rigaku UltraX18 generator and RAXIS DS3C). Here, the fiber was spun from the isotropic melt at 160 °C and subsequently annealed for 12 h at 130 °C, which is higher than the T_g of the PMMA block and lower than the T_i of the MCLCP block. The WAXD pattern showed an inner layer reflection with a spacing of 1.63 nm on the meridian and a broad outer reflection with a spacing around 0.45 nm split above and below the equator. These features are characteristic of the SmC_A phase of BB-5(3-Me) polyester, indicating that the BB-5(3-Me) segments in the block copolymer formed the SmC_A phase identical to that of the BB-5(3-Me) homopolymer.[14] The layer reflections appearing in the fiber axis direction demonstrate that the smectic layers lie perpendicular to the fiber axis.

The corresponding SAXS pattern shown in Figure 2b confirms that a well-ordered lamellar type microdomain structure is formed by the block copolymer. The pattern includes multiple sharp peaks on the meridian parallel to the fiber axis. The intensities of these peaks were averaged over azimuthal sectors of 10° on each side of the fiber axis and are plotted against the scattering vector q $(= 4\pi \sin \theta/\lambda)$ in Figure 3. As seen in Figure 3, the ratios of the q values at the scattering peaks are 1, 2, 3, 4, and 5, indicating the formation of a lamellar structure with the normal parallel to the fiber axis. The lamellar period is 21.9 nm. On heating to temperature above the T_i of the MCLCP block, the SAXS profile became poor, leaving only the first- and second-order reflections with a spacing of 18.0 nm on the meridian. It indicates that the lamellar morphology was sustained even between the liquid phases of BB-5(3-Me) and PMMA although the lamellar order decreased.

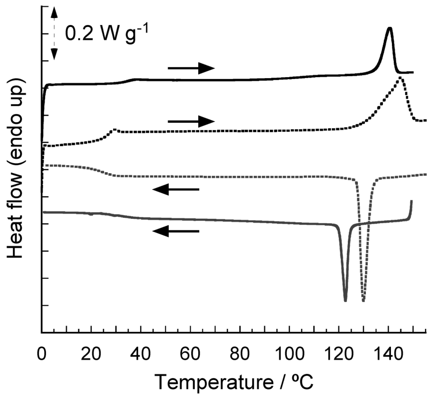

Figure 1. DSC thermograms observed for the hydroxy-terminated BB-5(3-Me) on (a) the second heating and (b) second cooling scans and those for the triblock copolymer on (c) second heating and (d) second cooling scans. Scanning rate was 10 °C min^{-1}.

The heights of successive scattering peaks are dependent characteristically on the reflection order: the first-, third-, and fifth-order reflections are relatively stronger than the second- and fourth-order ones. Such a feature of this scattering profile is associated simply with the relative ratio of the thicknesses of the two types of lamellae; hence, the thickness of each type of lamellae can be estimated by comparing the observed intensity $I_{obs}(q)$ with the scattering profile $I_{calc}(q)$ calculated on the basis of a pseudo-two-phase model with varying the lamellar thickness ratio. The scattering intensity of the lamellae can be calculated by the equation $I_{calc}(q) = \langle f^2\rangle - \langle f\rangle^2 + \langle f\rangle^2 Z(q)$, where f and $Z(q)$ are the structural factor for the pseudo-two-phase model[15−17] and the Fourier transform of the lattice-position distribution function with the second-type imperfection,[18,19] respectively (see Supporting Information). The most satisfactory profile can be produced by the model with a lamellar thickness ratio of 47:53 and the interface thickness of 0.75 nm. The electron density distribution along the lamellar normal is shown in Figure 4b. This lamellar thickness ratio is comparable with the volume ratio of PMMA and BB-5(3-Me) of 44:56, and the thickness of the LC lamella is hence determined to be 11.6 nm.

The LC lamellar thickness of 11.6 nm is much smaller than the contour chain length of the BB-5(3-Me) chain of 52 nm, suggesting that the MCLCP chains are folded to be accommodated in the LC lamella. The contour length equals to the product of DP = 32 and the smectic layer spacing (1.63 nm) because the MCLCP chain penetrates the smectic layers with most extended configuration. The parallel orientation of the smectic layers relative to the lamella let us depict the most stretched MCLCP segments extending from the interface but folding 3.4 times in order to be accommodated in the LC lamella as in Figure 4a. Such a folding of MCLCP has been discussed theoretically[20,21] and estimated experimentally.[22−30] The MCLCP segments of the block copolymer are thus folded at every seven repeat units like hairpin, and the folding sites locate at the boundary of the lamellae. Possibly, some extra repeat units of BB-5(3-Me) might be removed from the LC lamella into the amorphous PMMA region. It can be associated with the fact that

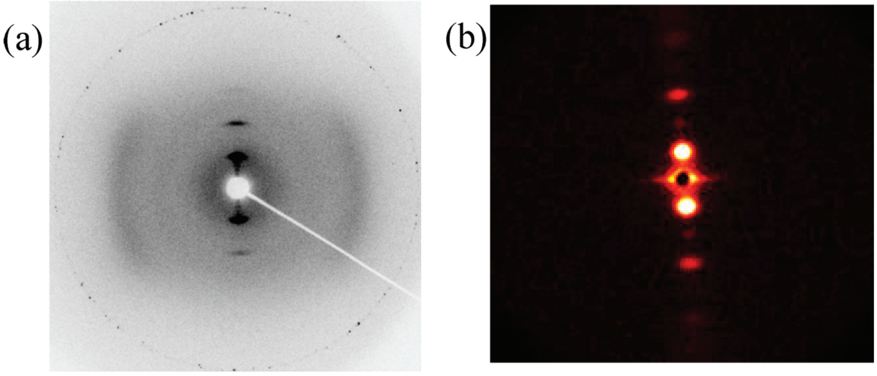

Figure 2. (a) WAXD and (b) SAXS patterns for the fiber sample of the triblock copolymer spun from the isotropic melt at 160 °C and annealed at 130 °C of the LC phase for 12 h. The fiber axis lies in the vertical direction.

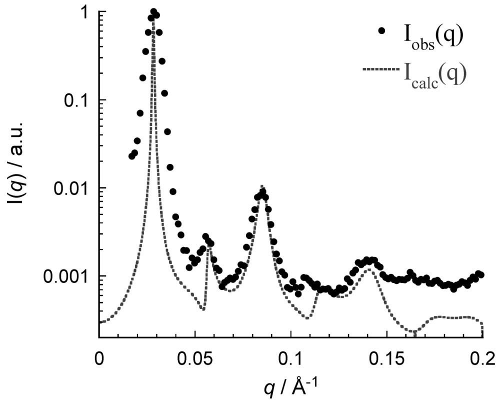

Figure 3. Normalized peak intensities of the SAXS pattern (closed circle) against the scattering vector q (= $4\pi \sin \theta/\lambda$). The dotted curve shows the calculated intensity based on the pseudo-two-phase model (see text).

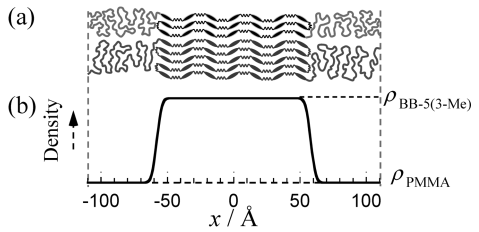

Figure 4. (a) A pseudo-two-phase model for the lamellar microphase-separated structure in which BB-5(3-Me) constructs uniform lamellae, assuming a hairpin folding at the interface. (b) The electron density profile satisfying the SAXS intensity profile.

ΔH_i of the MCLCP segments in the block copolymer is three-fourths of that observed for the precursor MCLCP. The fraction of the removed repeat units thus can be estimated to be less than 25%.

In summary, we successfully prepared an ABA triblock copolymer consisting of main-chain liquid crystalline BB-5(3-Me) polyester as the B block and PMMA as the A blocks by ATRP of MMA with a Br-terminated BB-5(3-Me) macroinitiator. The volume ratio of PMMA and BB-5(3-Me) segment was 44:56. The block copolymer showed a well-defined small-angle X-ray scattering pattern, which is attributed with the lamellar microdomain structure consisting of the SmCA BB-5(3-Me) and amorphous PMMA blocks. The thicknesses of the BB-5(3-Me) lamella was estimated as 11.6 nm, which is much smaller than the contour chain length (52 nm), meaning that the MCLCP segment folded 3.4 times on average. The MCLCP segments of the block copolymer are thus folded at every seven repeat units like hairpin so as to be accommodated in LC lamellae with a uniform thickness.

■ ASSOCIATED CONTENT

Ⓢ Supporting Information. Experimental details. This material is available free of charge via the Internet at http://pubs.acs.org.

■ ACKNOWLEDGMENT

This research was supported by a Grant-in-Aid for Creative Research from the Ministry of Education, Science, and Culture in Japan.

■ REFERENCES

(1) Osuji, C.; Ferreira, P. J.; Mao, G.; Ober, C. K.; Vander Sande, J. B.; Thomas, E. L. *Macromolecules* **2004**, *37*, 9903–9908.

(2) Tomikawa, N.; Lu, Z.; Itoh, T.; Imrie, C.; Adachi, M.; Tokita, M.; Watanabe, J. *Jpn. J. Appl. Phys.* **2005**, *44*, L711–L714.

(3) Adachi, M.; Takazawa, F.; Tomikawa, N.; Tokita, M.; Watanabe, J. *Polym. J.* **2007**, *39*, 155–162.

(4) Verploegen, E.; Zhang, T.; Jung, Y.; Ross, C.; Hammond, P. T. *Nano Lett.* **2008**, *8*, 3434–3440.

(5) Tokita, M.; Adachi, M.; Masuyama, S.; Takazawa, F.; Watanabe, J. *Macromolecules* **2007**, *40*, 7276–7282.

(6) Sänger, J.; Gronski, W.; Maas, S.; Stühn, B.; Heck, B. *Macromolecules* **1997**, *30*, 6783–6787.

(7) Anthamatten, M.; Zheng, W.; Hammond, P. T. *Macromolecules* **1999**, *32*, 4838–4848.

(8) Yamada, M.; Iguchi, T.; Hirao, A.; Nakahama, S.; Watanabe, J. *Macromolecules* **1995**, *28*, 50–58.

(9) Yamada, M.; Iguchi, T.; Hirao, A.; Nakahama, S.; Watanabe, J. *Polym. J.* **1998**, *30*, 23–30.

(10) Itoh, T.; Tomikawa, N.; Yamada, M.; Tokita, M.; Hirao, A.; Watanabe, J. *Polym. J.* **2001**, *33*, 783–791.

(11) Angeloni, A. S.; Bignozzi, M. C.; Laus, M.; Chiellini, E.; Galli, G. *Polym. Bull.* **1993**, *31*, 387–392.

(12) Wang, S. H.; Coutinho, F. M. B.; Galli, G.; Chellini, E. *Polym. Bull.* **1995**, *34*, 531–537.

(13) Fischer, H.; Poser, S. *Acta Polym.* **1996**, *47*, 413–428.

(14) Osada, K.; Koike, M.; Tagawa, H.; Tokita, M.; Watanabe, J. *Macromol. Chem. Phys.* **2004**, *205*, 1051–1057.

(15) Ruland, W. *Colloid Polym. Sci.* **1977**, *255*, 417–427.

(16) Ruland, W. *J. Appl. Crystallogr.* **1971**, *4*, 70–73.

(17) Hashimoto, T.; Kawai, T. *Macromolecules* **1977**, *10*, 377–384.

(18) Gunier, A. In *X-Ray Diffraction In Crystals, Imperfect Crystals, and Amorphous Bodies*; Dover Publications: San Francisco, 1994; p 295.

(19) Hosemann, R.; Baguchi, S. N. In *Direct Analysis of Diffraction by Matter*; North-Holland: Amsterdam, The Netherlands, 1962; p 302.

(20) de Gennes, P. G. In *Polymer Liquid Crystals*; Ciferri, A., Krigbaum, W. R., Meyer, R. B., Eds.; Academic Press: New York, 1982; p 122.

(21) Williams, D. R. M.; Warner, M. *J. Phys. (Paris)* **1990**, *51*, 317–340.

(22) Li., M. H.; Brulet, A.; Cotton, J. P.; Davidson, P.; Strazielle, C.; Keller, P. *J. Phys. II* **1994**, *4*, 1843–1863.

(23) Tokita, M.; Takahashi, T.; Hayashi, M.; Inomata, K.; Watanabe, J. *Macromolecules* **1996**, *29*, 1345–1348.

(24) Tokita, M.; Osada, K.; Watanabe, J. *Liq. Cryst.* **1997**, *22*, 453–456.

(25) Tokita, M.; Osada, K.; Yamada, M.; Watanabe, J. *Macromolecules* **1998**, *31*, 8590–8594.

(26) Tokita, M.; Tokunaga, K.; Funaoka, S.; Osada, K.; Watanabe, J. *Macromolecules* **2004**, *37*, 2527–2531.

(27) Tokita, M.; Tagawa, H.; Niwano, H.; Osada, K.; Watanabe, J. *Jpn. J. Appl. Phys.* **2006**, *45*, 1729–1733.

(28) Ishige, R.; Tokita, M.; Naito, Y.; Zhang, C.-Y.; Watanabe, J. *Macromolecules* **2008**, *41*, 2671–2676.

(29) Ishige, R.; Naito, Y.; Kang, S.; Tokita, M.; Watanabe, J. *Macromolecules* **2009**, *42*, 2557–2562.

(30) Ishige, R.; Tokita, M.; Funaoka, S.; Kang, S.; Watanabe, J. *Macromol. Chem. Phys.* **2011**, *212*, 48–54.